JOURNAL OF
EMERGING INVESTIGATORS

Article

Computational Study of Erosion Effects on a Triangular Aerofoil's Aerodynamics at Reynolds number of 10,000

Yilin Liuhan[1], Toby Bryce-Smith[2]
[1] Eton College, Windsor, Berkshire, United Kingdom
[2] Imperial College London, Greater London, United Kingdom

SUMMARY

Erosion has been shown to affect an aerofoil's performance at Reynolds numbers O~10^5-10^6, however, there is a lack of literature covering low-Reynolds-number aerofoils O~10^3-10^4. Therefore, we captured the effects of erosion on a triangular aerofoil's performance at a Re of 10,000 to assess erosion's impact on low-Re aerofoil robustness in harsh conditions, such as those experienced on Mars. We hypothesized that aerofoil performance, measured through lift and drag coefficients, would be sensitive to erosion location and form. We found that the leading and top edge were the most sensitive to changes, causing an augmentation of the suction surface's pressure gradient that affected performance more than trailing edge erosion. We further hypothesized that increasing erosion severity would amplify any trends observed. A two-dimensional steady computational fluid dynamics (CFD) simulation was created using a k-ω Shear-Stress-Transport (SST) model and a structured mesh with 55,460 cells. Results showed that erosion affects aerodynamic performance, with -35.2% to +23.2% change in lift and -16.0% to +28.8% change in drag across an angle of attack range of -3° to +6°. We found improved lift-to-drag ratios for angles of attack of more than +2° for top-edge erosion. Furthermore, data showed that top edge erosion provided the largest performance enhancement and trailing edge erosion the most performance lost. Aerofoil performance was highly sensitive to erosion location, causing independent trends that were typically amplified by erosion severity. This study showed that aerodynamicists must thoroughly assess the effects of erosion and damage on low-Re aerofoil performance to optimize aerofoil design.

INTRODUCTION

An aerofoil is the 2D cross-section of a structure intended to harness a lifting force owing to the flow of a fluid (either a liquid or a gas) over it. A fluid exerts a force on a structure through pressure differences and viscous forces, commonly vectorized into 'lift' and 'drag'. Aerodynamicists design lifting structures to maximize the lift-to-drag ratio to reach the highest efficiency possible. Aerofoils have different designs for different applications, from aircraft wings to wind turbine blades.

The flow physics around an aerofoil is largely dominated by Reynolds number (Re); a dimensionless value used to describe the ratio of viscous to inertial forces on a fluid flow, scaled by an object's size, the fluid velocity, and a fluid's parameters (density and viscosity). A fluid's force on a body is formed of frictional and pressure forces, therefore it follows that a changing Re will have a key influence on how fluids interact with structures. The effect of reducing Re below ~100,000 causes a significant decline in the ratio of lift to drag, owing to a complex change in the behavior of flow around the aerofoil. While this phenomenon provides no impact on the aerofoils of passenger aircraft and wind turbines, it does impact aerofoils that operate in low-density atmospheres (e.g. Mars), high viscosity fluids (e.g. water), and on small scales (e.g. insect wings). Low-Re aerofoils are gaining more interest owing to their development in new applications, such as micro-unmanned aerial vehicles (UAVs) on Earth, in sectors such as agriculture, to rotor aerofoils for Ingenuity, the first Martian helicopter (1, 2). Optimizing aerofoils improves overall efficiency, meaning the machines themselves can operate for longer or travel further, which reduces operating costs.

With the benefit of longevity comes the risk of performance deterioration due to unavoidable elements of their application; aerofoils have been shown to be affected by erosion across different applications, such as wind turbines. Previous studies have shown that erosion to the leading edge of wind turbine aerofoils caused performance degradation at 1-2 million Re (3) (**Figure 1**). The erosion led to a dramatic decrease in lift coefficient (Cl) as a function of the drag coefficient (Cd), highlighting a decrease in efficiency (3). Furthermore, wind turbines in sandy environments require regular maintenance to mitigate damage to the aerofoil leading edge due to erosion and bird strike (4). However, maintenance is not always possible, and, in these cases, aerofoils are designed to be robust to changes in geometry as seen in jet engines against the threat of foreign object debris (5). Assessment of the changes to aerofoil performance caused by erosion is therefore important for many applications.

The sandy Martian environment has already shown to be damaging to machinery sent in recent decades. Martian helicopter blades experience erosion from striking sand, especially during takeoff and landing (6). The sandstorms on Mars pose an additional level of erosion, which further changes the performance of aerofoils as sand particles change the surface and structure through erosion, abrasion, and impact damage (7). The low atmospheric density on Mars causes a decrease in flow Re which reduces the maximum lift-to-drag ratio achievable from an aerofoil and, therefore, peak performance. The aerofoil also needs to withstand unforeseen circumstances since sending vehicles to Mars is expensive. Ingenuity, the first Martian helicopter, cost $80 million to

https://doi.org/10.59720/24-260

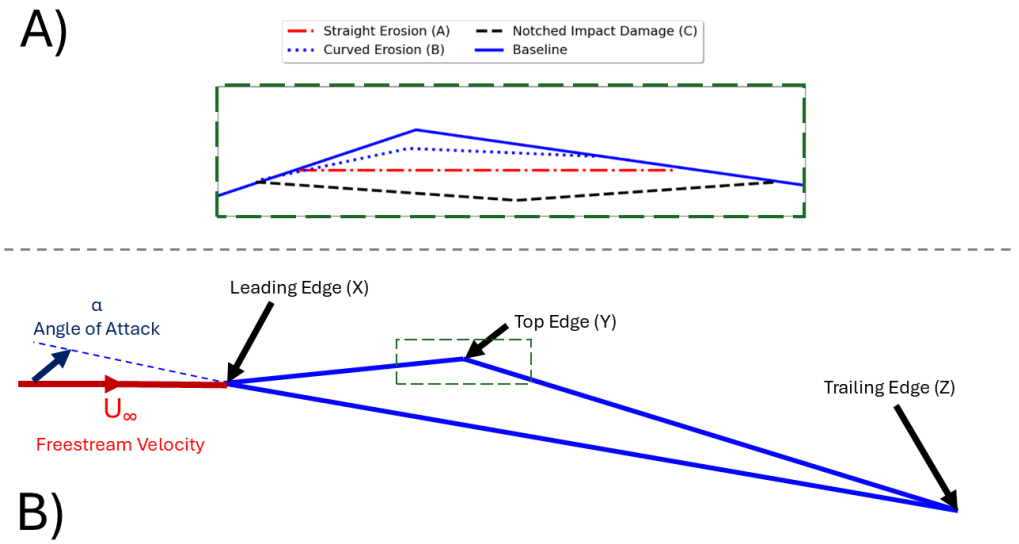

Figure 1: Nomenclature and visualization of erosion edits to the top-edge of the aerofoil used in the study. (A) Visualization of the three different erosion modes at the top edge: AY3, BY1, CY5 (170°), and the baseline aerofoil. AY3 represents impact damage, BY1 represents erosion damage, and CY5 represents impact damage. Note that edits have varying mass loss for clarity. (B) Visualization of the nomenclature used for the study and a representative green hatched box showing the location of the zoomed figure 1A on the larger aerofoil.

build, and Perseverance, the carrier of the Ingenuity, cost an additional $243 million (8). Furthermore, the journey to Mars can take from 9 to 21 months depending on the location of Mars relative to Earth. This means valuable time, money, and potential data are lost if the aerofoil is not built for withstanding erosion. With an additional emerging low-Re aerofoil application being an autonomous micro-UAVs in disaster recovery, the importance of assessing the impact of erosion on aerofoil performance is also of Earth-based importance. With an increasing interest in low-Re applications, an emerging interest in planetary missions such as the Martian helicopter, and a clear threat from erosion on aerofoil performance highlighted within high-Re literature, we focused on assessing the impact of erosion on an aerofoil's performance. We focused on the linear region of the lift curve, where the C_l increases linearly with angle of attack. We also collected an associated C_d to assess the 'cost' of lift generation. Drag in this region is non-linear, consisting of viscous drag and pressure drag. We avoided high angles of attack as this would increase the complexity of our numerical solver. Nonetheless, a focus on the linear region of the lift curve will encompass most design angles of attack used within industry, and our results can be extended to areas of high current academic interest such as bio-inspired corrugated aerofoils owing to the triangular aerofoil's geometric similarity.

The purpose of this investigation was to determine the effects of erosion and impact damage on the aerodynamic performance of a low-Re aerofoil such as those seen in Martian conditions. We hypothesized that erosion to the aerofoil's geometry would cause different performance augmentation based on location and severity of erosion as assessed through lift and drag coefficients, with location ultimately predicted to be the most sensitive parameter and erosion severity increasing observed changes. The boundary layer is more susceptible to separation at lower Re, thus a relocation and potential strengthening or depowering of suction surface pressure gradients owing to erosion location would have potentially more severe effects on the overall performance (9). Additionally, a changing erosion mode was tested as we further hypothesized that performance would be sensitive to the style of geometry change, although ultimately being less sensitive than erosion location. Our results largely support these hypotheses. In particular, we showed that performance was more sensitive to erosion location than mode, although most cases presented different effects as predicted. The results from this study can be transferred to other areas within the low-Re aerofoil literature, such as bio-inspired corrugated aerofoils.

RESULTS

A computational fluid dynamics (CFD) simulation was created to mimic Martian conditions at Re = 10,000. We used a triangular aerofoil to directly test the accuracy of this solver with experimental data. Multiple simulations were then run at different angles of attack to collect a lift curve and drag polar. These could then be compared for eroded aerofoils to show the effect of erosion on the aerofoil's performance.

The leading edge is highly susceptible to erosion due to its alignment to the particle-laden airflow. At this condition, changing the angle of attack made little difference compared to baseline except for AX5, which experienced a 23.2% increase in C_l compared to baseline at $\alpha = 3°$ (**Figure 2**). AX5 also experienced a 28.8% increase in C_d at $\alpha = 6°$. The other cuts remained close to the baseline except for at $\alpha = 6°$, where there was a 18.9%, 17.7%, 20.4% or 34.2% decrease in C_l for AX1, AX3, AX5 or BX1 respectively. BX3 and BX5 did not converge at $\alpha = 6°$; however, BX2 and BX5 achieved convergence at $\alpha = 5°$ and a similar decrease in C_l. The C_l/C_d ratio saw overall decrease except for BX5 at $\alpha = 3°$. The change in leading edge profile had the effect of slightly reducing the gradient of the linear portion of the lift curve slope, which combined with the lower C_l/C_d ratio, indicated a drop in performance.

The top corner is susceptible to erosion from the sand that is carried in the boundary layer as the blade moves through the

https://doi.org/10.59720/24-260

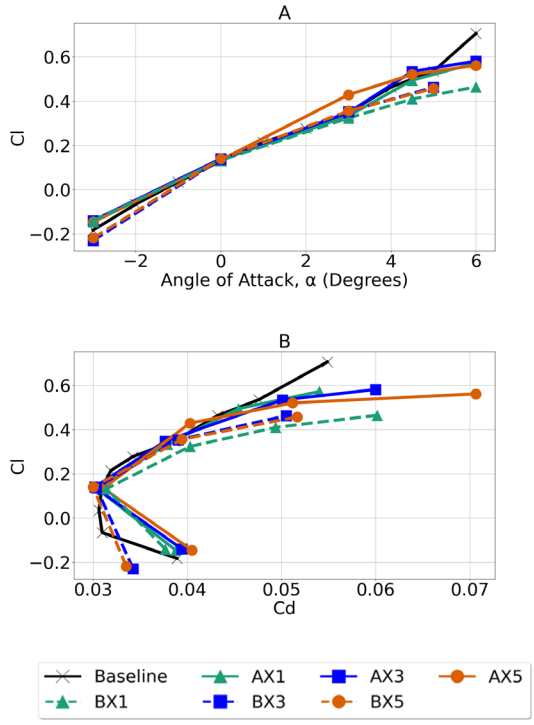

Figure 2: Different damage types on the leading edge and their effects on aerodynamic performance. The effect of leading edge erosion cases (denoted by X), on the (A) lift and (B) drag coefficients (Cl and Cd, respectively) at varying angles of attack.

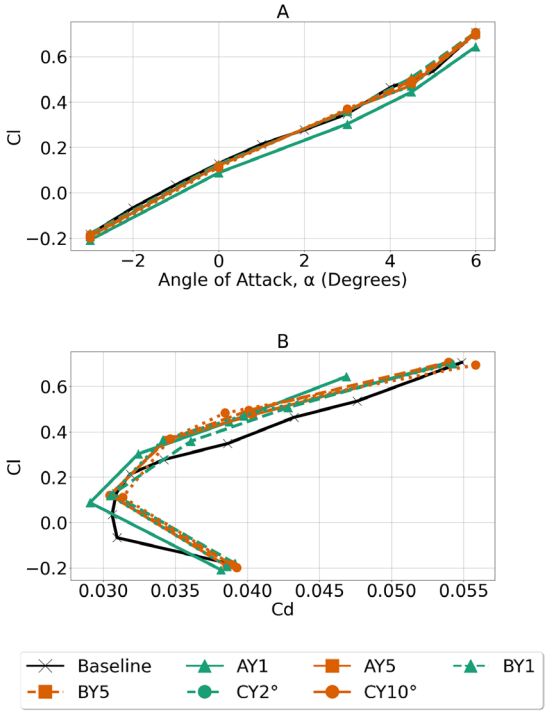

Figure 3: Different damage types on the top edge and their effects on aerodynamic performance. The effect of top edge erosion cases (denoted by Y) on the (A) lift and (B) drag coefficients (Cl and Cd, respectively) at varying angles of attack. AY3 and BY3 were omitted for clarity due to similarity with 1% and 5% variants.

air. The gradient of the lift curve slope became shallower for all cases except AY1, which maintained a similar trend but shifted to the right (**Figure 3**). AY1 was, however, an exception with the lift being 13.6%, 31.8%, 13.0% or 8.8% lower for α = -3°, α = 0°, α = 3° or α = 6°, respectively. The C_l/C_d ratio saw an overall increase for most of the cuts at all α and an increase for all edits after α = 2°. The corrugated cut producing the highest C_l/C_d at α = 0°or α = 3°, but performed similarly to the other top edge cuts at other angles of attack. AY1 is a significant outlier since its lift was on average 16.8% lower than baseline. The improvement for C_l/C_d was a result of the decrease in drag, likely caused by the thinning of the aerofoil which leads to less area for drag to act on and a narrower wake leading to reduced pressure drag. The lower cuts typically gave a slightly higher C_l and the curve cuts were slightly better for C_l against α and C_l as a function of C_d. The surface pressure comparison for top edge erosion showed an altered location of suction peak on the suction surface, causing a forward shift in adverse pressure gradient location (**Figure 4**). An implication of this, albeit directly not recorded, would be an earlier stall point as the angle of attack further increases.

The final stage of testing looked at erosion to the trailing edge, which saw the gradient of the lift curve slope diminished compared to the baseline aerofoil. The trailing edge edits reduced the gradient of the lift curve slope compared to the baseline (**Figure 5**). BZ1 and BZ3 at α = 3° were exceptions with the C_l being 13.4% and 4.4% higher than baseline. There was the same trend of a larger cut leading to lower lift at a decelerating rate, with the 1% cut seeing an initially large performance drop which then diminished for 3% and 5% cases. The curved cuts led to a better C_l/C_d ratio to the baseline for α > 0°. The straight-line cuts led to similar or lower C_l/C_d ratio compared to the baseline, likely due to the increased pressure drag through a wider wake.

DISCUSSION

The main observation was that all mass edits, even at 1% mass loss, caused notable shifts in aerofoil performance. Mass loss on each corner of the triangle aerofoil caused a performance change, although with different ramifications on the eroded aerofoil's relative performance. These differences are to be expected based on the unique flow physics at each location on the aerofoil, such as suction peaks in the vicinity of the leading edge and the adverse pressure gradient near the top edge. Individually, there were some patterns, such as an increase in mass loss, consistently leading to more drag at the leading edge. In contrast, drag consistently decreased as the top edge was eroded. Typically, changes were amplified as mass loss increased; however, this did not occur linearly, and anomalies exist, such as AY1, which did not obey this trend. Therefore, we have shown that erosion and impact damage affect aerodynamic performance, with unique trends for each erosion location as hypothesized. Contrary to the hypothesis, it is noted that performance changes with increasing erosion can be non-linear and, therefore, highlight greater complexity within the flow physics that should be explored further. A key possibility is shifting pressure gradients on the suction surface of the aerofoil, which could lead to non-linearities forming.

C_l is only notably affected by erosion at the leading and trailing edge. This is potentially from the eroded aerofoils having less chord length for the pressure force to act over, confirmed by results at the top edge where C_l was largely unchanged, and

https://doi.org/10.59720/24-260

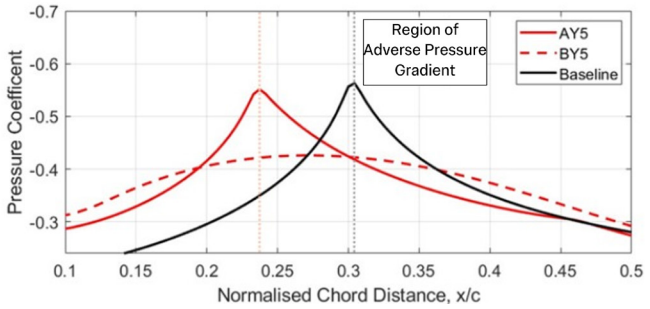

Figure 4: Contours of pressure coefficient over the suction surface of AY5, BY5, and baseline. The region of adverse pressure gradient is labelled. AY5 shows a forward shift in suction peak of roughly 0.07 c, denoted by vertical dotted lines. The magnitude of the suction peak decreases by ~24% for BY5.

the chord length is not changed by erosion. However, this is potentially more complex as shown by significant changes in the gradient of the lift curve slope at AX5 at α = 3° or AZ3 at α = 3°. The lack of change to C_l during top edge erosion may be caused by the triangle aerofoil being eroded into a flat plate, which is corroborated by the drop in drag.

All geometries saw a rapid drag increase at high angles of attack, independent of whether lower angle of attack performance showed an improvement or not compared to the baseline aerofoil. This was especially apparent at α = 6°, where almost all edited aerofoils had or trended towards having a worse C_l/C_d than the baseline. Erosion at the leading edge causes larger suction peaks on the aerofoil which increases the severity of the adverse pressure gradient, making the boundary layer more prone to earlier separation. This was seen in the reduction of gradient in the drag polar for these cases. The overall result follows the theory that at low-Re, a larger leading-edge radius makes the aerofoil more prone to flow separation (10). Results indicated that stalling behaviour may be significantly affected by erosion and should be investigated further to assess the impacts on aerodynamic stability.

Sensitivity to erosion style from the hypothesis was confirmed; however, with the added complexity that opposite trends are observed depending on location. For example, a curved edit produces less lift and more drag at the leading edge, and this reversed at the trailing edge. At the top edge, there was a minimal effect on lift, but a significant decrease in drag. The results indicated that aerofoil performance has some sensitivity to erosion mode, as predicted in the hypothesis; however, trends are not consistent in location. The top edge was also the only edit with consistent increase for C_l/C_d. At the leading and top edge, a larger cut meant more drag. This was the opposite for the trailing edge. The results indicate that the form of erosion has a notable effect and therefore should be considered in an aerodynamic design. CFD simulations will always have limitations stemming from the solver, the model, and the mesh. The solver did not always converge, for example at α = 6° in the case of BX3 and BX5. This inability to converge means that we cannot discuss higher angles of attack and therefore stall behavior. While errors compared to experimental data were acceptable, caution should always be taken with the interpretation of computational data, especially as minor changes to the mesh were required

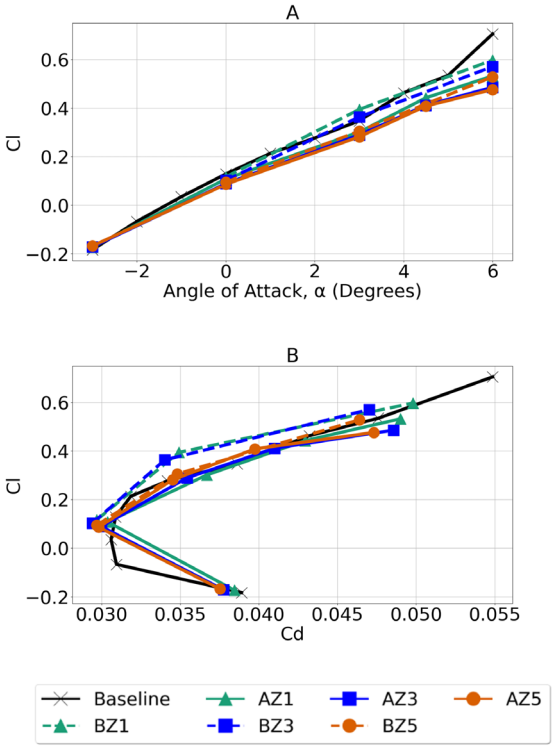

Figure 5: Different damage types on the trailing edge and their effects on aerodynamic performance. The effect of top edge erosion cases (denoted by Z) on the (A) lift and (B) drag coefficients (Cl and Cd, respectively) at varying angles of attack.

through different edits.

The results of our investigation have shown that erosion has a notable effect on aerofoil performance at three key locations on a triangular aerofoil. Based on these results, an aerodynamicist should take caution when designing a low-Re aerofoil for extreme conditions where erosion is a high risk, especially in areas that cause large performance shifts such as the leading edge. Additionally, erosion to the sharp corners will cause significant shifts in the pressure gradient on the suction surface. This result shows that a shift in stall behaviour is highly likely and should therefore be examined to outline safe operational margins to prevent sudden performance loss. This study should highlight to industry the need for testing of an aerodynamic surface's susceptibility to erosion early in the design process as even 1% mass loss shows significant shifts in the lifting efficiency of the tested aerofoil. A recommendation to industry from this study is that the potential erosion of a low-Re aerofoil should be explored as early as possible in the design stage in line with frameworks of Systems Engineering, to avoid unwanted performance augmentation. Engineering design should test the expected erosion in their environment early in the design process and then perform equivalent analysis to ensure either sufficient performance and safety margins are made or that material strengthening is applied to an aerofoil to reduce erosion.

Future works on this study in the field should seek to both develop understanding in the 2D setup and extend into further research questions. A steady Reynolds-averaged-Navier-Stokes simulation provides a brief exploration into the effects of turbulence on aerofoil performance, however, extension to a more direct turbulence solver such as Large Eddy Simulation

https://doi.org/10.59720/24-260

or even directly solving every turbulence scale using Direct Numerical Simulation, would enable turbulence at decreasing length scales to be resolved rather than modelled to enable a greater understanding of the underlying flow physics. An extension of this work to a 3D model would allow the investigation of spanwise stall behaviour. Additionally, heterogeneous erosion modes, such as erosion only at a one end of a wing, can be studied to further develop an idea of erosion's impact on aircraft performance. Results from this study can be extended to bio-inspired aerofoil research, such as corrugated aerofoils, which rely on sharp corners to improve performance, therefore benefiting from the geometric similarity within this study. Wing additives such as tubercles inspired by whale fins could also be assessed (16).

MATERIALS AND METHODS

Development of CFD Solver

ANSYS Fluent, a commercial CFD software, was used in this study (17). The experiment was created under Martian conditions, using an atmospheric density of 0.019 kg/m^3 and a dynamic viscosity of 9.8e-6 Ns/m3 (13). We used a freestream velocity of Mach 0.15 and a Re of 10,000 to validate our data against Suwa et al. who tested the performance of the triangle aerofoil in a Martian wind tunnel (14, 15). This then resulted in a chord length of 0.143 m, which was fixed throughout for the C_l and C_d calculations at the design value. The freestream velocity was also held constant at 36 m/s. We simulated angles of attack (denoted as α) from -3° to 6° in order to capture the linear region for the aerofoil. We used a k-ω SST turbulence model as this model combines the advantages of both k-ω and k-ε models, providing better accuracy for boundary layers with separation without the increased computational costs of higher fidelity turbulence models such as the Reynolds stress model or the shear stress transport model. This was done to find a balance of accuracy with the limited computational costs. We changed the domain physics of the fluid domain in order to make the solver as realistic as possible. In the configuration, from the default k-ω SST, we turned on a low-Re correction. We used the gamma algebraic transition model, as this is required at a Re of 10,000 to improve accuracy with respect to boundary layer transition. We doubled β*, a coefficient within the turbulence model, from the 0.09 default to 0.18, as tuning β* has been shown to reduce error in other studies and showed an improvement in accuracy during initial testing of the solver (18).

We determined the damage by percentage of area removed,

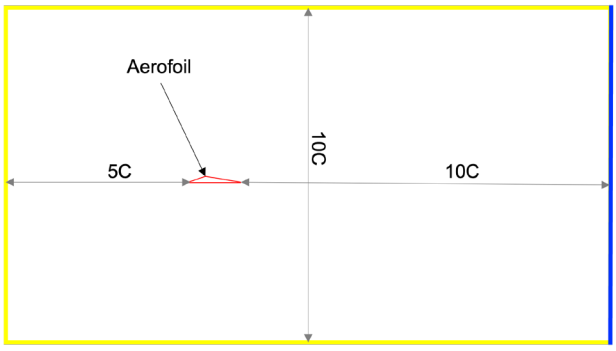

Figure 6: Computer Fluid Dynamics study setup diagram. Blue walls represent velocity outlets and yellow walls velocity inlets; the aerofoil is shown in red with C representing its chord length.

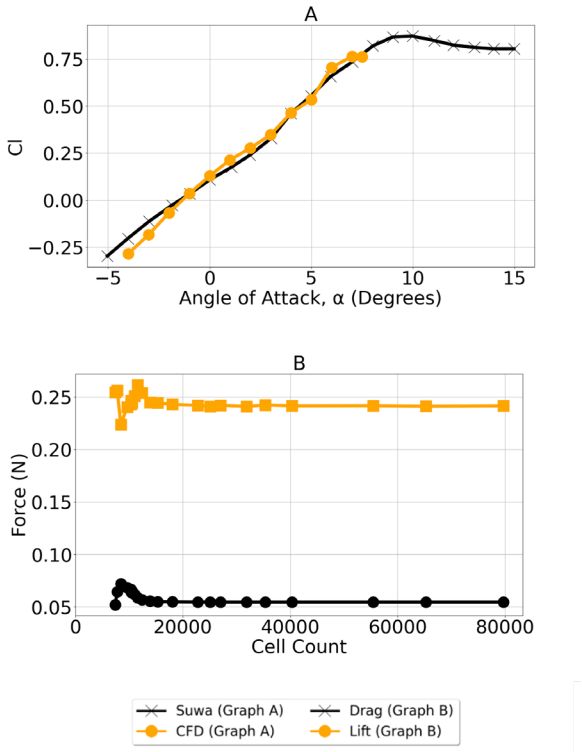

Figure 7: Data from the two validation studies performed on the CFD solver. (A) Lift curve slope from the validation study comparing CFD data to experimental data (15). (B) Lift force plots based on mesh cell count from the mesh convergence study.

at 1%, 3%, and 5% for the straight line and curved edits, and by the greatest angle of the isosceles triangle at 176°, 170°, and 160° for the notched edit. Different damage run cases are denoted as A, B or C for straight, curved or notched erosion, and X, Y or Z for leading, top or trailing edge. For the straight-line edits, we made a perpendicular cut to the base of the triangle for the leading edge and trailing edge and for the top edit, we made a cut parallel to the base of the triangle. The curved edits were made using the straight lines and adding a curved arc to it, adjusting for mass loss. The notched edits were made by using angle constraints on the top edge and moving the top edge down to resemble an M shape (**Figure 1**). Different geometry cuts were used to assess sensitivity to different erosion and damage type, with the curved edits mimicking erosion over time, and with straight and notched edits simulating sharp breaks from impact damage.

We used a structured mesh to improve solver accuracy. This was possible as the tested geometries were not too complex. The mesh was always visually checked for issues in cell aspect ratio to ensure discretisation errors were minimized. Additionally, the first cell size at the aerofoil surface was set to appropriately capture flow physics within the boundary layer. The domain was a rectangle with velocity inlets on the upstream and side walls (5 chord lengths tall), and a velocity outlet 10 chord lengths downstream (**Figure 6**). When aerofoil edits required, a curved wall was used instead to preserve a structured mesh. The downstream section of the domain was set to 10 chord lengths and the vertical distance from the aerofoil and the side walls were set as 5 chord lengths each side. We used 55,460 cells for

https://doi.org/10.59720/24-260

the baseline aerofoil, concluded from our mesh convergence study (**Figure 7**). If convergence was an issue at a specific aerofoil geometry, we doubled the cell count and rechecked the mesh quality while ensuring the solution converged. A solution was only accepted if residuals had finished decreasing and were all below a value of 10^{-4} for continuity residual and below 10^{-8} for all other residual values.

Assessing Solver Accuracy

A validation study was performed to assess the accuracy of the 2D CFD solver compared to experimental data from Suwa et al. (15). It was shown that mean error for the range of -4 to +8° was 20.1%, however, for positive angles of attack the percentage error was 7.7%, especially for 3° and above, the percentage error was 4.1% (**Figure 7A**). The solution diverged at angles of attack near where separation occurs; therefore, this study was limited to angles of attack between -3 and +6 degrees to ensure collected data was accurate. While errors exist when comparing to experimental data, it is worth noting differences exist on the computational side (in meshing quality and turbulence modelling) and the experimental side (in model surface roughness and background turbulence intensity) that will never lead to a perfect agreement. Owing to this, results from the solver should be looked at comparatively rather than as absolute values, reflected in our analysis.

To minimize the discretization error while minimizing solver time, a mesh convergence study was performed. This featured the gradual increase of the number of cells in the domain to note when the values of lift and drag outputted by the solver no longer changed. At the point where this plateaued, further refinement of the mesh was seen to increase computational time for negligible improvement in accuracy. In the mesh convergence study, the lift and drag values stabilized at around 35,000 cells so we made the simulations with at least 50,000 cells to give some room for error (**Figure 7B**).

Received: August 20, 2024
Accepted: October 30, 2024
Published: March 28, 2025

REFERENCES

1. Liu, Xu., et al. “Challenges and Opportunities for Autonomous Micro-UAVs in Precision Agriculture.” *IEEE Micro*, vol. 42, no. 1, 1 Jan. 2022, pp. 61–68. https://doi.org/10.1109/MM.2021.3134744.
2. “*Ingenuity Mars Helicopter.*” *NASA Science*. https://www.science.nasa.gov/mission/mars-2020-perseverance/ingenuity-mars-helicopter/. Accessed 17 Aug. 2024.
3. Sareen, Agrim., et al. “Effects of Leading Edge Erosion on Wind Turbine Blade Performance”. *Wind Energy*, vol. 17, no. 10, 3 Sep. 2014, pp. 1531–42. https://doi.org/10.1002/we.1649.
4. Wang, Xiaohang., et al. “Effect of Different Types of Erosion on the Aerodynamic Performance of Wind Turbine Airfoils.” *Sustainability*, vol. 14, no. 19, 28 Sep. 2022, pp. 12344. https://doi.org/10.3390/su141912344.
5. Yang, Pingping., et al. “Review of Damage Mechanism and Protection of Aero-Engine Blades Based on Impact Properties.” *Engineering Failure Analysis*, vol. 140, Oct. 2022, p. 106570. https://doi.org/10.1016/j.engfailanal.2022.106570.
6. Farrell, W. M., et al. “Will the Mars Helicopter Induce Local Martian Atmospheric Breakdown?” *The Planetary Science Journal*, vol. 2, no. 2, 10 Mar. 2021, pp. 46-54. https://doi.org/10.3847/PSJ/abe1c3.
7. Sagan, Carl. “Sandstorms and Eolian Erosion on Mars.” *Journal of Geophysical Research*, vol. 78, no. 20, 15 July 1973, pp. 4155–4161. https://doi.org/10.1029/JB078i020p04155.
8. “Ingenuity, NASA’s Mars Helicopter.” *The Planetary Society*. https://www.planetary.org/space-missions/ingenuity. Accessed 17 Aug. 2024.
9. Roberts, Luke S., et al. “Characteristics of Boundary-Layer Transition and Reynolds-Number Sensitivity of Three-Dimensional Wings of Varying Complexity Operating in Ground Effect.” Journal of Fluids Engineering, vol. 138, no. 9, 3 June 2016, https://doi.org/10.1115/1.4033299.
10. Koning, Witold J., et al. “Optimization of Low Reynolds Number Airfoils for Martian Rotor Applications Using an Evolutionary Algorithm.” *AIAA Scitech 2020 Forum*, 5 Jan. 2020. https://doi.org/10.2514/6.2020-0084.
11. Boiko, Andrey V., et al. “Physics of Transitional Shear Flows. Fluid Mechanics and Its Applications.” 1st ed, vol. 98, Springer Nature, 2012, pp. 33-36
12. Wakeling, J. M., and Ellington, C. P. “Dragonfly Flight: I. Gliding Flight and Steady-State Aerodynamic Forces.” *Journal of Experimental Biology*, vol. 200, no. 3, Feb. 1997, pp. 543–556. https://doi.org/10.1242/jeb.200.3.543.
13. Bardera, Rafael., et al. “Aerodynamics of Mars 2020 Rover Wind Sensors.” *Mars Exploration - a Step Forward*, 19 Mar. 2020. https://doi.org/10.5772/intechopen.90912.
14. “Sounds of Mars.” *NASA Science*. https://science.nasa.gov/mission/mars-2020-perseverance/sounds-of-mars/. Accessed 17 Aug. 2024.
15. Suwa, Tetsuya., et al. “Compressibility Effects on Airfoil Aerodynamics at Low Reynolds Number.” *30th AIAA Applied Aerodynamics Conference*, June 2012, https://doi.org/10.2514/6.2012-3029.
16. “Whale-Inspired Wind Turbines.” *MIT Technology Review*. https://www.technologyreview.com/2008/03/06/221447/whale-inspired-wind-turbines/. Accessed 17 Aug. 2024.
17. “Ansys® Student 2024 R2, Free Student Software Downloads.” *Ansys Inc*. https://ansys.com/academic/students. Accessed 21 Oct. 2024.
18. Younoussi, Somaya., and Ettaouil, Abdeslem. “Calibration Method of the K-ω SST Turbulence Model for Wind Turbine Performance Prediction near Stall Condition.” *Heliyon*, vol. 10, no. 1, 15 Jan. 2024, https://doi.org/10.1016/j.heliyon.2024.e24048.